Research on the support of larger broken gateway based on the combined arch theory

Hongyun Yang[*1,2], Yanbao Liu[3], Yong Li[**2], Ruikai Pan[2], Hui Wang[2],
Feng Luo[4], Haiyang Wang[1] and Shugang Cao[2]

[1]*State Key Laboratory of Mountain Bridge and Tunnel Engineering, Chongqing Jiaotong University, Chongqing, 400074, China*
[2]*State Key Laboratory of Coal Mine Disaster Dynamics and Control, Chongqing University, Chongqing 400044, China*
[3]*China Coal Technology Engineering Group Chongqing Research Institute, Chongqing 400039, China*
[4]*School of Mining and Geomatics, Hebei University of Engineering, Handan, Hebei, 056038, China*

Abstract. The excavation broken zones (EBZ) of gateways is a significant factor in determining the stability of man-made opening. The EBZ of 55 gateways with variety geological conditions were measured using Ground Penetrating Radar (GPR). The results found that the greatly depth of EBZ, the smallest is 1.5 m and the deepest is 3.5 m. Experimental investigations were carried out in the laboratory and in the coal mine fields for applying the combined arch support theory to large EBZ. The studies found that resin bolts with high tensile strength and good bond force could provide high pretension force with bolt extensible anchorage method in the field. Furthermore, the recently invented torque amplifier could greatly improve the bolt pretension force in poor lithology. The FLAC3D numerical simulation found that the main diffusion sphere of pretension force was only in the free segment zone of the surrounding rock. Further analysis found that the initial load-bearing zone thickness of the combined arch structure in large EBZ could be expressed by the free segment length of bolt. The using of high mechanical property bolts and steel with high pretension force will clearly putting forward the bolt length selection rule based on the combined arch support theory.

1. Introduction

The surrounding rock stability of gateway is a major concern in underground coal mines and the ground failure conditions of gateways depending on stress, geological and geotechnical conditions. The research of failed mechanisms has been a major focus in the field of coal mining (Xu *et al.* 2019, Wang *et al.* 2019, Yang *et al.* 2020). To date, studies have developed a deeper understanding, including the compressive stress failure types, tensile stress failure types, shear stress failure types, squeezing and fluidity failure types, as well as geological structure failure types. Based on the failure mechanisms, many active support models have been suggested, while the combined supporting technology using bolt, mesh, and cable was found very effective for ground control.

In related research fields, considerable studies are turning to the failure range of the surrounding rock (Yang *et al.* 2016). Due to gateway failure range plays a significant role in determining the support parameters of the surrounding rock, and efforts on this subject have been discussed by many researchers (Gu and Ozbay 2015, Dong

et al. 1994, Pusch and Stanfors 1992, Renaud *et al.* 2011). Terms describing different failure ranges have been defined by many as causes (Tsang *et al.* 2005, Sato *et al.* 2000, Zhang *et al.* 2019). At present, the definitions of intact zones, excavation plastic zones (EPZ) and excavation broken zones (EBZ) are employed for study, as shown in Fig. 1(Yang *et al.* 2016, Zhao *et al.* 2019, Wang *et al.* 2015, Renaud *et al.* 2011, Yuan *et al.* 2018).

The intact zone is the intact surrounding rock with an in situ stress state. The EPZ is defined as a zone without major changes in flow, transport properties that develop with micro-fracturing, and an integrated structure with a certain carrying capacity for deep coal and rock mass. Thus, the EPZ is not the key zone needed to control in order to obtain stability of coal and rock mass that surrounds gateways (Tsang *et al.* 2005, Sato *et al.* 2000). The EBZ is defined as a zone with major changes in flow and transport properties that develop with macro-fracturing; its size plays a significant role in the stability around man-made openings, which has been sparked deep discussion and research by Dong *et al.* (Dong *et al.* 1994), Wang *et al.* (2015), Tsang and Bernier (Tsang *et al.* 2005), and so on. Moreover, Ground Penetrating Radar (GPR) techniques are proposed to obtaining the EBZ width. GPR is a non-destructive method that provides a relatively quick geophysical measurement and is widely used for testing various engineering structures, obtaining crack distribution characteristics and broken widths in a test location, and its advantages are superior to other methods (Pérez-Gracia *et*

∗Corresponding author, Professor
  E-mail: yanghy@cqu.edu.cn
∗∗Co-Corresponding author, Professor
  E-mail: yong.li@cqu.edu.cn
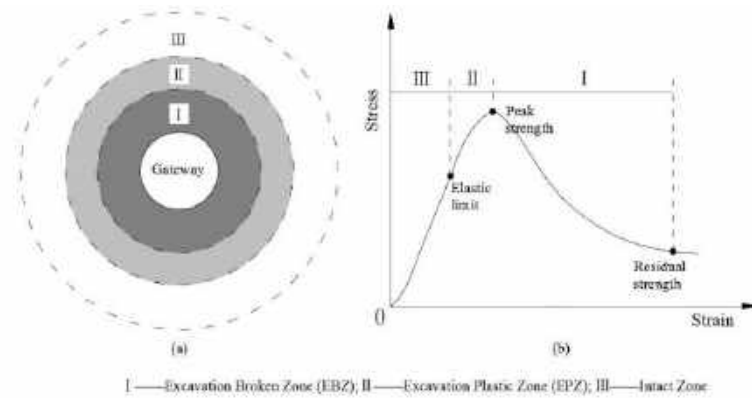
Fig. 1 Surrounding rock failure mode of gateway (a) schematic diagram of failure zone and (b) failure zone in the view of a stress-strain curve obtained by triaxial compression tests

al. 2008, Xiang *et al.* 2013, McCann and Forde 2001, Orbán and Gutermann 2009, Zhang *et al.* 2012, Song *et al.* 2002).

Moreover, the combined support technology mentioned above plays an important role in gateway EBZ control, and has realized that pretension force in bolts plays a decisive role. Because the pretension force bolt with the surrounding rock can form a "stress arch" bearing structure (Carranza-Torres 2009), the active supporting role of bolt and the self-bearing capacity of the structure were given full play. Furthermore, Lang (1961) made a classic "broken rock anchorage test", and vividly explained the bolt reinforcement effect. Therefore, research in the distribution rules of pre-stress in surrounding rock, the formation condition of compressive stress zones, the range of anchoring zones has an important theoretical significance and engineering application value, and many scholars contributed to this research direction. Gu *et al.* (2000) studied the influence of pretension force and bolt length on the stress distribution zones around the bolt by a similarity simulation experiment. Kang *et al.* (2014) summed up the engineering experience, a FLAC3D numerical simulation and similarity simulation method, and studied the support effect and action mechanism of pretension force bolt, the distribution form and influencing factors of pre-stress fields in surrounding rock. Lin *et al.* (2016) analyzed the distribution characteristics of the pre-stress field of a single end anchorage bolt from a large model test, found that two concentration zones of compressive stresses formed near the two ends of free segments and a concentration zone of tensile stress formed near the anchorage segments. Guo *et al.* (2013) researched the distribution of the stress field under the condition of end anchorage bolts with circular trays based on the elastic theory. Showkati *et al.* (2015) studied the distribution of stress fields in the surrounding rock which contained vertical joints under the condition of end anchorage bolts. Ranjbarnia *et al.* (2014) studied the distribution of stress fields in a circular roadway with pretension force bolt by full length anchorage, and analyzed the influence of pretension force and bolt density on that stress field. Ding *et al.* (2002) and Wang *et al.* (2008), useing a FLAC3D numerical simulation, studied the stress distribution characteristics in surrounding rock supported by pretension force cable. Wei and Li (Wei and Li 2013)

adopting a FLAC3D numerical simulation studied the formation factors of the anchorage body in the use of pretension force bolt and the destabilization mechanisms resulting from the in-situ stress.

Many scholars investigated stress field and its influencing factors, and obtained numerous achievements using diverse methods. However, most of the experiments were conducted by using several bolts or a single bolt with low pretension force. Kang *et al.* (Kang 2016) pointed out that the bolt pretension force range is usually between 30 kN to 90 kN at present, and when pretension force exceed 100 kN, the surrounding rock could obtain a good support effect. For further understanding of the anchor action mechanism and the continuous improvement of bolt material parameters and support technologies, many new insights should be discovered. This paper analyzes the support effects of high pretension force bolts on an EBZ, based on the combined arch theory. Section 2 provides the GPR test results of gateways broken width. Section 3 conducts experimental studies on the improved material parameters of bolts in the laboratory and in the field to prove its ability to provide high pretension force. Section 4 evaluates its presented support theory of an EBZ and analyzes the initial load-bearing zone of gateway surrounding rock and the selection principle of bolt support design parameters. Sections 5 and 6 summarizes the paper with discussions and conclusions.

2. Test of gateways broken width

2.1 Introduction of test fields

The investigation fields are distributed over a large area, and the test coal mines are located in five mining areas (denoted areas 1, 2, 3, 4 and 5) in Sichuan Province, China, as shown in the satellite image in Fig. 2. There are 19 coal mines including 55 typical gateways in total (Yang *et al.* 2016).

Geological factors around the extracted gateways mainly include the dip angle and thickness of coal seams, the immediate roof and buried depth. Due to severe geological movements geological conditions are complex according to the data in Table 1 (Yang *et al.* 2016). The key
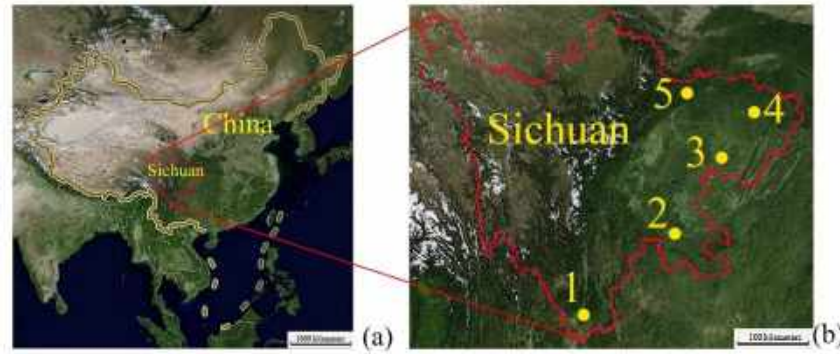
Fig. 2 Investigated fields (a) and (b) the location of the test coal mines, in Sichuan Province, China

Table 1 Geological conditions parameters of test gateways

Conditions	Dip angle of coal seam/(°)	Thickness of coal seam/(m)	Thickness of immediate roof/(m)	Buried depth/(m)
minimum	9	0.5	less than 1	approximately 200
maximum	67	close to 5	approximately 18	approximately 700
most	25-40	0.8-2.5	3-6	300-500
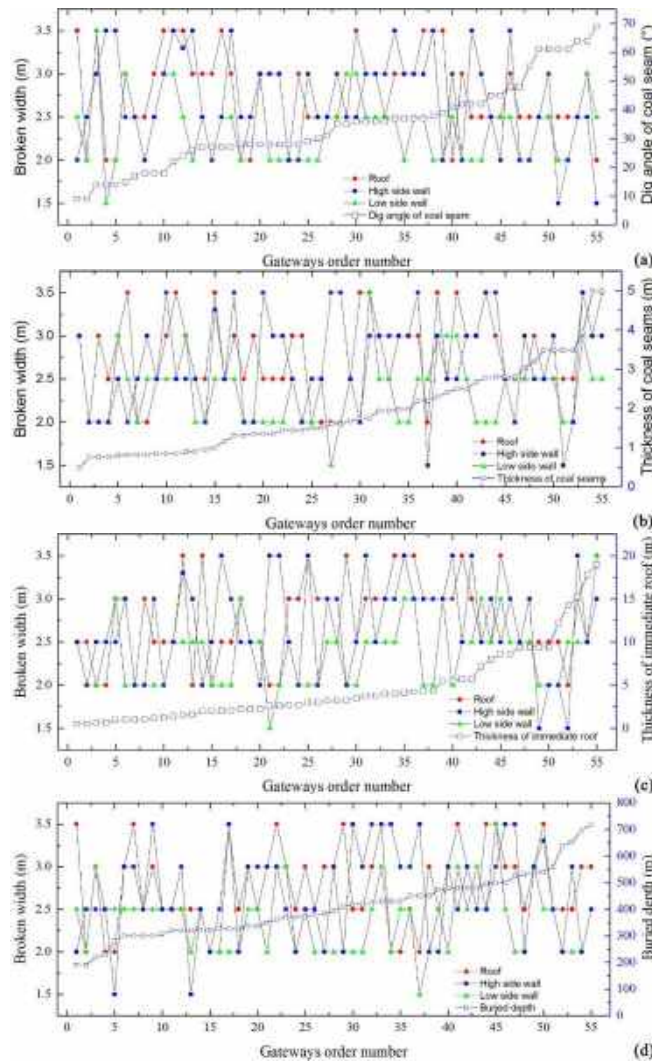
Fig. 3 Broken width and the geological conditions of tested gateways (a) relationship between the broken width and dip angle of coal seams, (b) relationship between the broken width and thickness of coal seams, (c) relationship between the broken width and thickness of immediate roof and (d) relationship between the broken width and buried depth

factors influence the broken width had large variable ranges.

The test locations were in advanced roadways of head entry or tail entry beyond the front abutment pressure zone, and in the original rock stress zones and under static pressure, where the roof and roadway walls did not have large deformation and did not need to reinforced support.

2.2 Results of gateways broken width

Test principle of GPR can reference (Yang *et al.* 2016). After working with GPR, 55 typical gateways broken widths were tested, including the high-wall of roadway, low-wall of roadway, and roof. To analyze the relationship between the broken width and the gateway geological factors, the gateways were numbered from 1-55, arranged in order of the value of geological factors from small to large, as shown in Fig. 3. It can be observed from the broken widths that the broken widths of the tested gateways were large, the minimum value was 1.5 m, and the maximum value was 3.5 m; and the broken width in the roof and high wall were generally greater than that in the low wall.

Combined with the broken width and the geological conditions for the mines, the following conclusions were obtained, and other analyses for reasons can reference (Yang *et al.* 2016, Sarfarazi *et al.* 2018, Lee and Hong 2018, Yin *et al.* 2018).

(1) As seen in Fig. 3(a), for coal seams with a small dip angle, the broken widths in the roof were larger, as seen in gateways Numbered 7-17. For a large dip angle of the coal seam, the broken widths in the roof were smaller, which was evident in gateways Numbered 18-28 and 45-55.

(2) As seen in Fig. 3(b), for the relatively larger thicknesses of the coal seam, the broken width in the roof and the high side wall were larger; conversely, failures were relatively small, which was more obvious among the gateways Numbered 50-55.

(3) As seen in Fig. 3(c), for the relatively smaller thicknesses of the coal seam, the broken widths in the roof and the high side wall were smaller, particularly between gateways Numbered 1-10. As the thickness of the immediate roof become larger, for gateways Numbered 50–55, the broken width had the tendency of increasing because the immediate roof had lower strength than the main roof.

(4) As seen in Fig. 3(d), the smaller the buried depth, the smaller the broken width, which were obviously reflected among gateways Numbered 1-15. For gateway Numbered 37, the buried depth was relatively large, consequently the broken width was large. A few gateways in front of gateway Numbered 37 had small buried depths and small broken widths.

3. Experimental studies on the improved material parameters of bolts

For the EBZ support, many scholars (Wang *et al.* 2015, Zheng *et al.* 2012) believed that bolt anchorage length and the amount of bolt pretension force play important roles in controlling the surrounding rock. Kang *et al.* (Kang 2016)
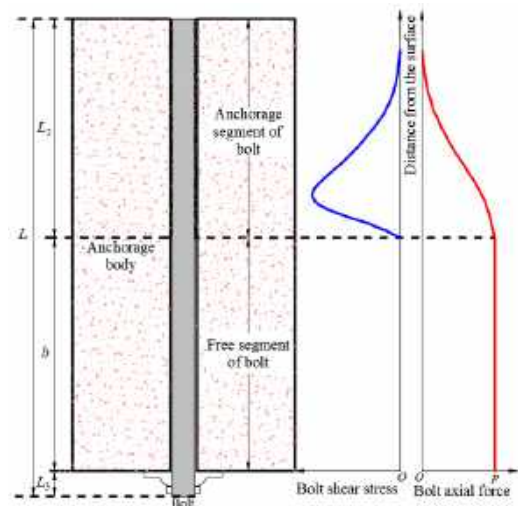
Fig. 4 Force distribution diagrammatic sketch of an anchorage body and bolt

pointed out that when pretension force exceeds 100 kN, the surrounding rock can obtain a good support effect. To conduct an experimental investigation to test whether the mechanical properties of bolts, such as tensile strength and anchorage force, can provide high pretension force which is more than 100 kN. It must firstly discuss the anchorage length of a bolt and its mechanical effects.

3.1 Mechanical effects of a bolt with pretension force

After theoretical research, the results of a bolt pretension force mechanical effects were obtained in Fig. 4 (Wang *et al.* 2015, Zheng *et al.* 2012, Zhou *et al.* 2015, Ma *et al.* 2013, Nemcik *et al.* 2014, Li *et al.* 2014). It suggested that: (1) the bolt in the anchored segment has a peak shear stress and rapid decay after peak value and the increase of the pretension force cannot lead to the pretension force in an anchored segment spreading to deeper surrounding rock; (2) the increase of the pretension force can improve the pretension force peak in an anchorage body and compressive stress on the surface of the surrounding rock; (3) the bolt's axial force (pretension force) in the free segment remains about the same, but there is a sharp decay in the anchored segment, unable to spread to a deeper bolt. It means the blot pretension force almost works on the free segment of rock mass and had little effect on an anchored segment (anchorage length of bolt) of rock mass. Thus, the anchorage length of a bolt should be carefully determined.

There are three kinds of anchorage methods in terms of the anchorage length (Kang 2016): (1) when the anchorage length is not greater than 500 mm or 1/3 of the borehole length for the bolt, it is called end anchorage; (2) when the anchorage length is not less than 90% of the borehole length for the bolt, it is called full length anchorage; (3) when the anchorage length is between the length of an end anchorage and a full length anchorage, it is called extensible anchorage. Further analysis reveals that: (1) the dispersion range of pretension force of a bolt with full length anchorage is minimum relative to the other two anchorage methods; in addition, the jumbolter often stop running

Table 2 Testing results of the mechanical properties of bolts

Number	Yield load (kN)	Yield strength (MPa)	Breaking load (kN)	Breaking strength (MPa)	Percentage elongation (%)
1	255	671	306	805	18.2
2	250	658	303	797	19.5
3	254	668	304	800	Over gauge length
4	249	655	300	789	Over gauge length
Average value	252	663	304	798	18.8

Fig. 5 Fracture surface of tensile broke bolts

Fig. 6 Cross-section of anchored segment (a) anchorage length of 300 mm and (b) anchorage length of 125 mm

Fig. 7 The nut status when the bolt load was 300 kN

during stiring bolt with resin cartridge when the bolt was using full length anchorage; (2) the bolt with end anchorage can increase the dispersion range of pretension force, but the anchorage length is shorter, resulting in low safety coefficiency to a bolt in a large EBZ, and the bolt will lose efficacy easily under an action of high pretension force.

Therefore, based on the above analysis, the extensible anchorage method was determined to best support the gateway surrounding rock with a large EBZ (Wang *et al.* 2015, Zheng *et al.* 2012, Wang *et al.* 2019).

3.2 The improved mechanical performance of a bolt

Anchorage force is a useful indicator to assess the support system, and is dependent upon the complicated geological engineering factors and loading conditions to which it is subjected (Li *et al.* 2014). The strength parameters of the bolt itself, the bond force at the interface between the bolts and the rock, and the surrounding rock property, as well as the bearing capacity of the load point on the surface are all primary factors found in previous studies. Field results, using high-performance steel in the rock bolt, show the load bearing capacity on a surface is reliable, and will be not discussed in this paper. Hence, this section will analyze whether the current industrial technology can provide high pretension force under the mentioned another three primary factors.

3.2.1 Bolt pullout test

For the purpose of investigating the mechanical properties of a bolt used in an extensible anchorage method, the strength parameters of the bolt itself should first be tested. Hence, four hot-rolled fine thread resin bolts with a diameter of 22 mm and a length of 2400 mm were static pull tested. The results are listed in Table 2, and the bolt fracture surface was shown in Fig. 5.

The average values of yield load, breaking load and percentage elongation are 252 kN, 304 kN and 18.8% respectively, indicating the strength parameters of this type
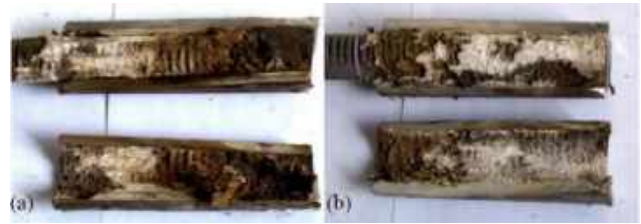
of bolt have significantly increased compared to many previously used bolts with a tensile breaking strength of 100 to 150 kN in coal mines (Kang 2016, Li *et al.* 2014). They are characterized by their high load capacity.

3.2.2 Bond force test in a laboratory

In addition to the strength parameters of the bolt itself, the bond force of the grouted part is also a useful factor to reflect the anchorage force. Two kinds of anchorage lengths of bolts mentioned above were laboratory tested to investigate the capability of providing suitable bond force. The results are listed in Table 3, and parts of the cross-section of anchored segment are shown in Fig. 6.

It observed that sliding failure occurred at the bolt interface of the tube. The average anchorage force of a bolt with an anchorage length of 300 mm could reach up to 249.5 kN, almost equals to the tensile strength of the bolt. It is much higher than that of a bolt with an anchorage length of 125 mm. Therefore, it is reasonable to believe that when the anchorage length is longer than 300 mm of extensible anchorage, the anchorage force will increase. It also reflects that the resin cartridge of MK Φ2835 has superior performance and can provide a higher bond force. In addition, the hot-rolled fine thread resin bolt not only has a higher anchorage force in a laboratory, but also has a self-locking effect. It can be seen that the matching nut did not retreat after it locked the bolt when the loading force reached 300 kN in the testing process, as shown in Fig. 7.

3.2.3 Anchorage force tests in the field

Laboratory tests on bolts can represent the behavior of bolts when applying a load at one end of the bolt. However, they cannot reproduce the field conditions and the actual rock mass state.

Field tests can provide quantitative data to examine the performance of rock mass supports. Hence, anchorage force pullout experiments were conducted in an immediate roof of a gateway in the field. The lithology of the immediate

Table 4 The pullout results of bolt anchorage force in field tests

Test position of bolt	Near gob/coal wall	Distance from heading end (m)	Anchorage force (kN)	Comment
Roof first row	Gob/ the second bolt	12.8	88	Not pullout enough
Roof second row	Gob/ the second bolt	12.2	132	Sleeve is snapped
Roof fifth row	Gob/ the third bolt	8.8	88	Not pullout enough
Roof sixth row	Coal wall/ the second bolt	8.0	88	Not pullout enough

Fig. 8 The sleeve used in a pullout test in the field

(a)   (b)

Fig. 9 Torque amplifier and torque wrench used in the field (a) torque amplifier and (b) torque wrench

roof at the test site was poor, containing sandy mudstone and coal streaks, with a thickness of 3.32 m, and the uniaxial compressive strength is less than 20 MPa. The dimensions of the bolts tested were: 22 mm diameter, 2400 mm length and 1500 mm anchorage length (extensible anchorage). The results are listed in Table 4.

The highest anchorage force was 132 kN when the sleeve snapped, parts of the sleeve in the field tests are shown in Fig. 8. On the other hand, it is reasonable to expect that the poor lithology could provide a higher anchorage force than 132 kN in the field when experiencing a bolt breaking or a bolt sliding failure.

3.2.4 Method for increasing pretension force

The above studies revealed that the bolt, resin cartridge and poor lithology have the ability to bear high pretension force. But, it is a question of how to conveniently increase the pretension force in the field. Thus, engineers invented a torque amplifier, which can make the bolt's original torque increase 3-3.5 times, greatly improving the bolt pretension force (Zou *et al.* 2015). Moreover, the torque size can be tested by digital display torque wrench. The torque amplifier and digital display torque wrench using in field were shown in Fig. 9.

Therefore, it can be seen that high pretension force can

be provided in the field to support the surrounding rock in a large EBZ by using the improved bolt and extensible anchorage method.

4. Support effect analyses of bolt and surround rock

4.1 Support theory assessment of gateways broken zones

For large broken widths, bolts installed within an EBZ can form a combined arch structure in the surrounding rocks. The support design should be adjusted to utilize the self-bearing capacity of the combined arch, and the support parameters design mainly depends on the combined arch theory (Wang *et al.* 2015). Previous research (in 1994) considered the bolt support parameter calculation diagram of a combined arch as shown in Fig. 10 (Dong *et al.* 1994), and the thickness of a combined arch could be determined by

$$b = \left(L \tan\beta - a\right)/\tan\beta \qquad (1)$$

where b is the thickness of a combined arch, L is the bolt's effective length, β is the bolt control angle in an EBZ which usually has the value of 45°, a is the inter-row spacing of bolts. To improve the bearing capacity of a combined arch in a large EBZ, it is necessary to increase the strength and thickness of the combined arch. Further study proposed the thickness of a combined arch is the basic parameter to calculate the bearing capacity of a combined arch, and with an increase in the thickness of a combined arch at a certain range, its bearing capacity would increase (Yu *et al.* 2010).

It was noted that the support parameter-calculation method in Eq. (1) was proposed under the condition that a bolt with low tensile strength, low anchoring force, and low pretension force (usually reflecting a passive support). Afterwards, with the invention of the high tensile strength resin bolt and steel and mesh, and the development of active support technology for pretension force bolt, the parameter selection of Eq. (1) should be discussed as follows:

(1) Under the action of bolt pretension force and high strength steel to its dispersion on the surface of the surrounding rock, whether the control angle of β is still 45°.

(2) The bolt usually was full-length anchored, whether it effectively increased the thickness of a combined arch, and formed a self-bearing structure.

(3) The thickness of a combined arch b was usually
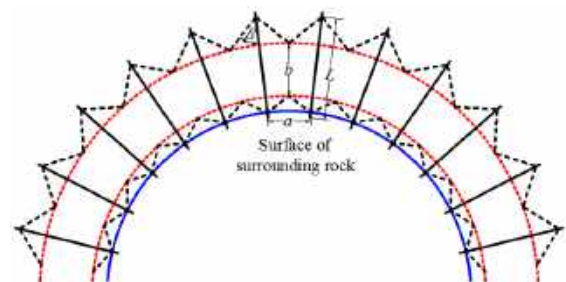
Fig. 10 Parameter calculation diagram of combined arch
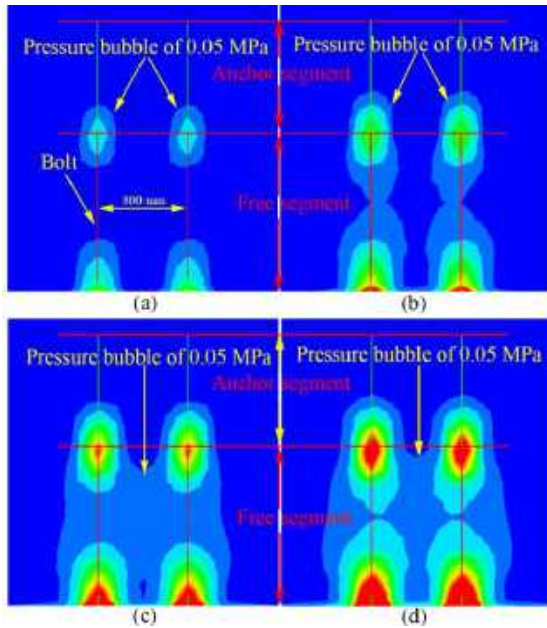
Fig. 11 Stress distribution contours in surrounding rock (a) pretension force of 30 kN, (b) pretension force of 60 kN, (c) pretension force of 90 kN and (d) pretension force of 120 kN

determined by an experience of 0.85 m, 0.9 m, 1 m, 0.9 m with different sizes.

Therefore, aiming at the above problems, it is very necessary to conduct further analyses on the combined arch support theory for a large EBZ according to modern bolt mechanical properties and numerical simulation technologies.

4.2 Stress diffusion analysis for anchored rock mass

In general, bolts and steel are used together. Thus, high pretension force bolt, high strength steel and extensible anchorage method were used to study the improving effect of a combined arch in a large EBZ, and the finite differential method of a FLAC3D was employed as the analytical tool (Jiang *et al.* 2016, Zhao *et al.* 2018, Haghnejad *et al.* 2018, Tian *et al.* 2019, Oh *et al.* 2019).

To reach a deeper understanding of the diffused characteristics of pretension force in surrounding rock when the rock bolt pretension force increases, pretension forces of 30 kN, 60 kN, 90 kN and 120 kN were used and calculated. Moreover, the numerical model utilized the Mohr-Coulomb failure criterion, and one sandstone material was endowed with the physical and mechanical parameters: elastic modulus of 30 GP, Poisson's ratio of 0.3, a density of 2400 kg/m^3, a cohesion of 10 MPa, a friction Angle of 30°, and tensile strength of 2 MPa. Simultaneously, the steel was endowed with elastic material, with an elastic modulus of 100 GP and a Poisson's ratio of 0.25. In addition, two bolts, with a diameter of 22 mm, a length of 2400 mm and an inter space of 800 mm, were used for the study. It must be emphasized that the anchorage length of 1000 mm was used and the bolt end was anchored with 10 mm to simulate bolt plate.

(a)

(b)

(c)

(d)
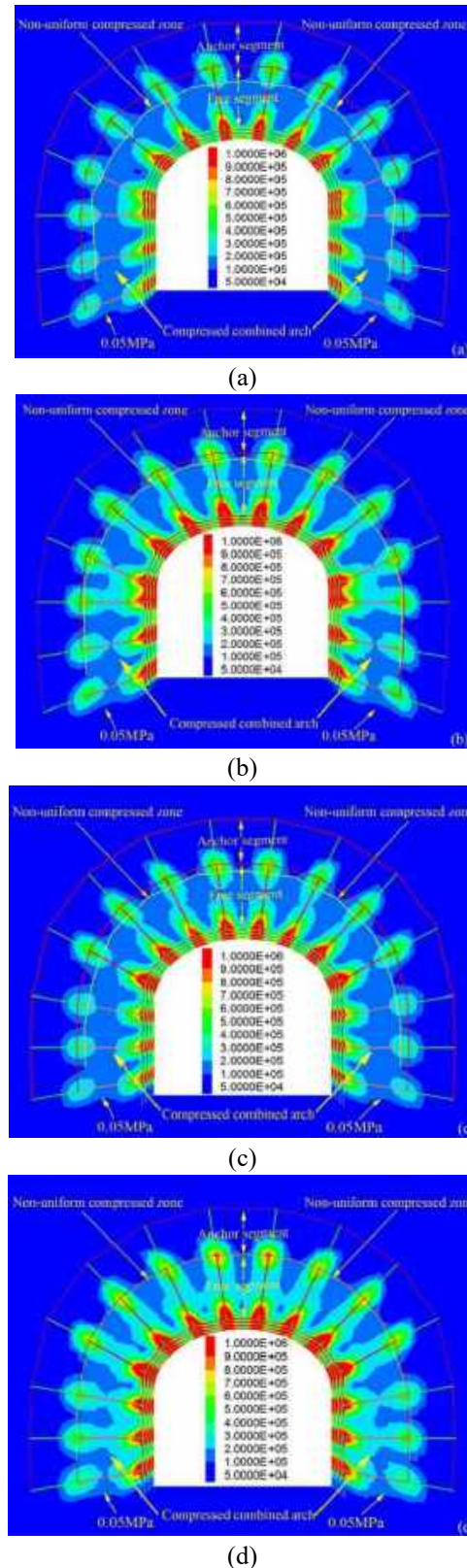
Fig. 12 Total stress distribution contours of anchored rock under different pre-tensioned force with steel belt: (a) bolts with inter-row spacing of 800 mm and pretension force of 90-120 kN, (b) bolts with inter-row spacing of 800 mm and pretension force of 120-150 kN, (c) bolts with inter-row spacing of 700 mm and pretension force of 90-120 kN and (d) Bolts with inter-row spacing of 700 mm and pretension force of 120-150 kN

Furthermore, the rock bolts were represented as built-in "cable" elements. For resin-grouted rock bolts, a stiffness of 2×10^{10} N/m/m, a cohesive strength of 4×10^{8} N/m, a friction angle of 33°, a cross-sectional area of 3.8×10^{-4} m^2, an elastic modulus of 205 GPa, a tensile yield strength of 250 kN were assigned to the "cable" element in this study. The calculation results are as shown in Fig. 11.

It is said that when the compressive stress value is greater than 0.05 MPa in rock mass, the rock mass is effectively controlled by bolt anchorage force (Wang *et al.* 2015). Fig. 11 schematically shows that:

(1) With the increase of pretension force, the range of pressure bubble of 0.05 MPa increases. First, the pressure bubbles began to connect in free segments in one bolt when the pretension force was 60 kN. Second, the pressure bubbles connected between bolts when the pretension force was 90 kN. Finally, the connected area had no further increase when the pretension force is 120 kN.

(2) Under the action of steel and pretension force, the pressure bubble almost distributed within the rock mass of the bolt free segment, illustrating that the initial extrusion reinforcement range was in the rock mass of the bolt free segment.

4.3 Initial load-bearing zone of gateway surrounding rock

The initial distribution area of the combined arch embodied the load-bearing capacity in a gateway surrounding rock under the action of bolt high pretension force. This section will study the initial load-bearing zone, and a gateway with an arched cross section as the calculation example, and with the above numerical model parameters of FLAC3D as the material. The following statistics were documented: (1) bolt inter-row spacing of 800 × 800 mm, bolt pretension force of 90 kN in two side walls and 120 kN in the arch crown with steel; bolt pretension force of 120 kN in two side walls and 150 kN in the arch crown with steel. (2) bolt inter-row spacing of 700 × 700 mm, bolt pretension force of 90 kN in two side walls and 120 kN in the arch crown with steel; bolt pretension force of 120 kN in two side walls and 150 kN in the arch crown with steel. The calculated results of the initial load-bearing zone in surrounding rock is shown in Fig. 12.

It is necessary to define the concept of a non-uniform compressed zone (NUCZ) that distributes between the anchor segment end and the combined arch surface, as shown in Fig. 12. Moreover, it shows other information:
(1) When the bolt inter-row spacing remains constant and with the increase of bolt pretension force, the NUCZ decreases and the thickness of the combined arch increases;
(2) When the bolt pretension force remains constant, and with the decrease of bolt inter-row spacing, the NUCZ decreases and the thickness of the combined arch increases;
(3) The sum of NUCZ and thickness of the combined arch is the free segment range, and with the increase of bolt pretension force and the decrease of bolt inter-row spacing, the NUCZ is close to zero, presenting that the free segment of anchorage body is the initial load-bearing zone (combined arch area).

The thickness of the initial load-bearing zone of gateway surrounding rock is the length of bolt free segment, as shown in Fig. 4. Thus, the thickness of combined arch b is equal to the bolt full length L_1 minus the bolt anchorage length L_2 and the bolt end exposed length L_3, as shown in $b = L_1 - L_2 - L_3$.

Furthermore, it can reference (Yu *et al.* 2010) to calculate the initial bearing capacity of a combined arch in a large EBZ. Therefore, the bolt with high pretension force will provide high bearing capacity to surrounding rock, and prevent large deformation and failure at the beginning of the bolt installation. It has remarkable advantages relative to the bolt with no steel and low bolt pretension force in surrounding rock

5. Discussion

The size of an anchorage force is an important parameter of evaluating rock bolt support capability in previous practical engineering. As mentioned above, the anchorage force is usually the rated anchorage force which is mainly dependent on the resin bonding strength and bolt tensile strength and because of the improvement of the supporting technology and material properties, the rated anchorage force is greater than the initial bolt pretension force. However, only when the surrounding rock experiences severe deformation, even failure, and the bolt tensile force is greater than the initial pretension force, the rated anchorage force will be exerted. The rated anchorage force is a passive support force.

On the other hand, the rock bolt initial pretension force is provided by a worker when the surrounding rock has no or small deformation and can be thought of as active support force. Furthermore, the support effect for gateway surrounding rock is reflected in whether using active support pretension force in a timely manner to make a combined arch work and increase its bearing capacity, but not reflected in whether the bolt tensile force or bond force reaches the rated the anchorage force.

Therefore, it can use the maximum initial pretension force which can be provided by an anchorage system (including resin bonding strength, bolt tensile strength, surrounding rock property, the bearing capacity of the load point on the surface, and so on) in an EBZ to evaluate the support capacity, but not the anchorage force.

6. Conclusions

Though the 55 gateways broken zone tests in surrounding rock with GPR, it was found that the minimum value was 1.5 m, and the maximum value was 3.5 m, the EBZ is large; and the broken widths in the roof and high side wall were relatively large compared to those in the low side wall. To make a further analysis of the combined arch support theory for large EBZ according to modern bolt mechanical properties and numerical simulation technology, we conducted experimental investigations in a laboratory and in the field. It found that the hot-rolled fine thread resin

bolt had high tensile strength presenting superior mechanical properties. Moreover, the pullout experiment illustrated that the poor lithology can provide high anchorage force with a bolt extensible anchorage method. Finally, the invented torque amplifier can greatly improve bolt pretension force, and meet high pretension force support requirement.

In addition, after a FLAC3D numerical simulation analysis, it found that the pretension force main diffusion sphere was in the free segment zone of the surrounding rock. Further analysis showed that the initial load-bearing zone thickness of a combined arch structure in a large EBZ can be expressed by the bolt free segment length, when using high mechanical property bolts and steel with high pretension force, and finally, clearly put forward the bolt length selection rule based on the combined arch support theory.

Acknowledgments

References

Carranza-Torres, C. (2009), "Analytical and numerical study of the mechanics of rockbolt reinforcement around tunnels in rock masses", *Rock Mech. Rock. Eng.,* **42**(2), 175-228. http://doi.org/10.1007/s00603-009-0178-2.

Ding, X., Sheng, Q., Han, J., Cheng, L. and Bai, S. (2002), "Numerical simulation testing study on reinforcement mechanism of prestressed anchorage cable", *Chin. J. Rock Mech. Eng.*, **21**(7), 980-988.

Dong, F., Song, H., Guo, Z., Lu, S. and Liang, S. (1994), "Roadway support theory based on broken rock zone", *J. China Coal. Soc.*, **19**, 21-32.

Gu, J., Shen, J., Chen, A. and Ming, Z. (2000), "Model testing study of strain distribution regularity in rock mass caused by prestressed anchorage cable", *Chin. J. Rock Mech. Eng.*, **S1**, 917-921.

Gu, R. and Ozbay, U. (2015), "Numerical investigation of unstable rock failure in underground mining condition", *Comput. Geotech.*, **63**, 171-182. https://doi.org/10.1016/j.compgeo.2014.08.013.

Guo, X., Mao, X., Ma, C. and Huang, J. (2013), "Bolt support mechanism based on elastic theory", *Int. J. Min. Sci. Technol.*, **23**(4), 469-474. https://doi.org/10.1016/j.ijmst.2013.07.002.

Haghnejad, A., Ahangari, K., Moarefvand, P. and Goshtasbi, K. (2018), "Numerical investigation of the impact of geological discontinuities on the propagation of ground vibrations", *Geomech. Eng.*, **14**(6), 545-552. https://doi.org/10.12989/gae.2018.14.6.545.

Jiang, L.S., Sainoki, A., Mitri, H.S., Ma, N.J., Liu, H.T. and Hao, Z. (2016), "Influence of fracture-induced weakening on coal mine gateroad stability", *Int. J. Rock Mech. Min. Sci.*, **88**, 307-317. http://doi.org/10.1016/j.ijrmms.2016.04.017.

Kang, H. (2016), "Sixty years development and prospects of rock bolting technology for underground coal mine roadways in China", *J. China U. Min. Technol.*, **45**(6), 1071-1081.

Kang, H.P., Jiang, P.F. and Cai, J.F. (2014), "Test and analysis on stress fields caused by rock bolting", *J. China Coal Soc.*, **39**(8), 1521-1529. http://doi.org/10.13225/j.cnki.jccs.2014.9019.

Lee, J. and Hong, J.W. (2018), "Crack initiation and fragmentation processes in pre-cracked rock-like materials", *Geomech. Eng.*, **15**(5), 1047-1059. https://doi.org/10.12989/gae.2018.15.5.1047.

Li, C.C., Stjern, G. and Myrvang, A. (2014), "A review on the performance of conventional and energy-absorbing rockbolts", *J. Rock Mech. Geotech. Eng.*, **6**(4), 315-327. http://doi.org/10.1016/j.jrmge.2013.12.008.

Lin, J., Shi, Y., Sun, Z., Wang, Z. and Cai, J. (2016), "Large scale model test on the distribution characteristics of the prestressed field of end-anchored bolts", *Chin. J. Rock Mech. Eng.*, **35**(11), 2237-2247. http://doi.org/10.13722/j.cnki.jrme.2016.0626.

Ma, S., Nemcik, J. and Aziz, N. (2013), "An analytical model of fully grouted rock bolts subjected to tensile load", *Constr. Build. Mater.*, **49**, 519-526. http://doi.org/10.1016/j.conbuildmat.2013.08.084.

McCann, D.M. and Forde, M.C. (2001), "Review of NDT methods in the assessment of concrete and masonry structures", *NDT E Int.*, **34**(2), 71-84. http://doi.org/10.1016/S0963-8695(00)00032-3.

Nemcik, J., Ma, S., Aziz, N., Ren, T. and Geng, X. (2014), "Numerical modelling of failure propagation in fully grouted rock bolts subjected to tensile load", *Int. J. Rock Mech. Min. Sci.*, **71**, 293-300. http://doi.org/10.1016/j.ijrmms.2014.07.007.

Oh, J., Moon, T., Canbulat, I. and Moon, J. (2019), "Design of initial support required for excavation of underground cavern and shaft from numerical analysis", *Geomech. Eng.*, **17**(6), 573-581. https://doi.org/10.12989/gae.2019.17.6.573.

Orbán, Z. and Gutermann, M. (2009), "Assessment of masonry arch railway bridges using non-destructive in-situ testing methods", *Eng. Struct.*, **31**(10), 2287-2298. http://doi.org/10.1016/j.engstruct.2009.04.008.

Pérez-Gracia, V., García García, F. and Rodriguez Abad, I. (2008), "GPR evaluation of the damage found in the reinforced concrete base of a block of flats: A case study", *NDT E Int.*, **41**(5), 341-353. http://doi.org/10.1016/j.ndteint.2008.01.001.

Pusch, R. and Stanfors, R. (1992), "The zone of disturbance around blasted tunnels at depth", *Int. J. Rock Mech. Min. Sci. Geomech. Abstr.*, **29**(5), 447-456. http://doi.org/10.1016/0148-9062(92)92629-Q.

Ranjbarnia, M., Fahimifar, A. and Oreste, P. (2014), "A simplified model to study the behavior of pre-tensioned fully grouted bolts around tunnels and to analyze the more important influencing parameters", *J. Min. Sci.*, **50**(3), 533-548. http://doi.org/10.1134/S1062739114030156.

Renaud, V., Balland, C. and Verdel, T. (2011), "Numerical simulation and development of data inversion in borehole ultrasonic imaging", *J. Appl. Geophys.*, **73**(4), 357-367. http://doi.org/10.1016/j.jappgeo.2011.02.007.

Sarfarazi, V., Haeri, H. and Shemirani, A.B. (2018), "Simulation of fracture mechanism of pre-holed concrete model under Brazilian test using PFC3D", *Smart Struct. Syst.*, **22**(6), 675-687. https://doi.org/10.12989/sss.2018.22.6.675.

Sato, T., Kikuchi, T. and Sugihara, K. (2000), "In-situ experiments on an excavation disturbed zone induced by mechanical excavation in Neogene sedimentary rock at Tono mine, central Japan", *Eng. Geol.*, **56**(1-2), 97-108 http://doi.org/10.1016/S0013-7952(99)00136-2.

Showkati, A., Maarefvand, P. and Hassani, H. (2015), "Stresses induced by post-tensioned anchor in jointed rock mass", *J. Central South Univ.*, **22**(4), 1463-1476. http://doi.org/10.1007/s11771-015-2664-x.

Song, H., Wang, C. and Jia, Y. (2002), "Principle of measuring broken rock zone around underground roadway with GPR and its application", *J. China U. Min. Tech.*, **4**, 43-46.

Tian, Z.H., Liu, J., Wang, X.G., Liu, L.P., Lv, X.B. and Zhang, X.T. (2019), "Deformation and failure mechanism exploration of surrounding rock in huge underground cavern", *Struct. Eng. Mech.*, **72**(2), 275-291. https://doi.org/10.12989/sem.2019.72.2.275.

Tsang, C.F., Bernier, F. and Davies, C. (2005), "Geohydromechanical processes in the excavation damaged zone in crystalline rock, rock salt, and indurated and plastic clays—in the context of radioactive waste disposal", *Int. J. Rock Mech. Min. Sci.*, **42**(1), 109-125. http://doi.org/10.1016/j.ijrmms.2004.08.003.

Wang, H., Jiang, Y., Xue, S., Shen, B., Wang, C. and Lv, J. (2015), "Assessment of excavation damaged zone around roadways under dynamic pressure induced by an active mining process", *Int. J. Rock Mech. Min. Sci.*, **77**, 265-277. http://doi.org/10.1016/j.ijrmms.2015.03.032.

Wang, H.T., Li, S.C., Wang, Q., Wang, D.C., Li, W.T., Liu, P., Li, X.J. and Chen, Y.J. (2019), "Investigating the supporting effect of rock bolts in varying anchoring methods in a tunnel", *Geomech. Eng.*, **19**(6), 485-498. https://doi.org/10.12989/gae.2019.19.6.485.

Wang, J., Kang, H. and Gao, F. (2008), "Numerical simulation study on load transfer mechanisms and stress distribution characteristics of cable bolts", *J. China Coal Soc.*, **33**(1), 1-6.

Wang, X., Kang, H. and Gao, F. (2019), "Numerical investigation on the shear behavior of jointed coal mass", *Comput. Geotech.*, **106**, 274-285. https://doi.org/10.1016/j.compgeo.2018.11.005.

Wei, S.J. and Li, B.F. (2013), "Anchor bolt body formation and instability mode under the influence of anchoring pretension", *J. China Coal Soc.*, **38**(12), 2126-2132. https://doi.org/10.13225/j.cnki.jccs.2013.12.018.

Xiang, L., Zhou, H.L., Shu, Z., Tan, S.H., Liang, G.Q. and Zhu, J. (2013), "GPR evaluation of the damaoshan highway tunnel: A case study", *NDT E Int.*, **59**, 68-76. http://doi.org/10.1016/j.ndteint.2013.05.004.

Xu, G., He, C. and Chen, Z. (2019), "Mechanical behavior of transversely isotropic rocks with non-continuous planar fabrics under compression tests", *Comput. Geotech.*, **115**, 103175. https://doi.org/10.1016/j.compgeo.2019.103175.

Yang, H., Cao, S., Li, Y., Fan, Y., Wang, S. and Chen, X. (2016), "Assessment of excavation broken zone around gateways under various geological conditions: A case study in Sichuan province, China", *Minerals*, **6**(3), 72. https://doi.org/10.3390/min6030072.

Yang, H.Y., Liu, Y.B., Cao, S.G., Pan, R.K., Wang, H., Li, Y. and Luo, F. (2020), "A caving self-stabilization bearing structure of advancing cutting roof for gob-side entry retaining with hard roof stratum", *Geomech. Eng.*, **21**(1), 23-33. https://doi.org/10.12989/gae.2020.21.1.023.

Yin, D.W., Chen, S.J., Chen, B., Liu, X.Q. and Ma, H.F. (2018), "Strength and failure characteristics of the rock-coal combined body with single joint in coal", *Geomech. Eng.*, **15**(5), 1113-1124. https://doi.org/10.12989/gae.2018.15.5.1113.

Yu, W., Gao, Q. and Zhu, C. (2010), "Study of strength theory and application of overlap arch bearing body for deep soft surrounding rock", *Chin. J. Rock Mech. Eng.*, **29**(10), 2134-2142.

Zhang, B., Li, Y., Fantuzzi, N., Zhao, Y., Liu, Y.B. and Peng, B. (2019), "Investigation of the flow properties of CBM based on stochastic fracture network modeling", *Materials*, **12**(15). https://doi.org/10.3390/ma12152387.

Zhang, P., Li, Y., Zhao, Y. and Guo, L. (2012), "Application and analysis on structure exploration of coal seam by mine ground penetrating radar", *Proceedings of the 2012 14th International Conference on Ground Penetrating Radar*, Shanghai, China, June.

Zhao, T., Zhang, Y, B., Zhang, Q. and Tan, Y. (2018), "Analysis on the creep response of bolted rock using bolted burgers model", *Geomech. Eng.*, **14**(2), 141-149. https://doi.org/10.12989/gae.2018.14.2.141.

Zhao, Y., Cao, S., Shang, D., Yang, H., Yu, Y. and Li, Y. (2019), "Crack propagation and crack direction changes during the hydraulic fracturing of coalbed", *Comput. Geotech.*, **111**, 229-242. https://doi.org/10.1016/j.compgeo.2019.03.018.

Zhao, Y., Cao, S., Yong, L., Zhang, Z. and Pan, R. (2018), "The occurrence state of moisture in coal and its influence model on pore seepage", *Rsc. Adv.*, **8**(10), 5420-5432. https://doi.org/10.1039/c7ra09346b.

Zheng, X.G., Zhang, N. and Xue, F. (2012), "Study on stress distribution law in anchoring section of prestressed bolt", *J. Min. Saf. Eng.*, **29**(3), 365-370.

Zhou, H., Xu, R.C., Zhang, C.Q., Lu, J.J., Meng, F.Z. and Shen, Z. (2015), "Research on effect of interior bonding section length of prestressed anchor rod", *Rock Soil Mech.*, **36**(9), 2688-2694. https://doi.org/10.16285/j.rsm.2015.09.032.

Zou, D., Li, M., Gong, L., Hu, Y. and Yang, H. (2015), "Study on the rib spalling and the treatment during driving in strong outburst and medium thick coal seam", *Coal Min. Mod.*, **4**, 81-83. http://doi.org/10.13606/j.cnki.37-1205/td.2015.04.035.

CC